An *Escherichia coli* nitrogen starvation response is important for mutualistic coexistence with *Rhodopseudomonas palustris*

Alexandra L. McCully[1], Megan G. Behringer[2], Jennifer R. Gliessman[1], Evgeny V. Pilipenko[3] Jeffrey L. Mazny[1], Michael Lynch[2], D. Allan Drummond[3], James B. McKinlay[1#]

[1]Department of Biology, Indiana University, Bloomington, IN

[2]School of Life Sciences; Biodesign Center for Mechanisms of Evolution, Arizona State University, Tempe, AZ.

[3]Department of Biochemistry & Molecular Biology; Department of Human Genetics, University of Chicago, Chicago IL.

Running title: Nitrogen starvation response in a bacterial mutualism

[#]Corresponding author. 1001 E 3rd Street, Jordan Hall, Bloomington, IN 47405

Phone: 812-855-0359

Email: jmckinla@indiana.edu

Conflict of interest.

The authors declare no conflict of interest

Abstract

Microbial mutualistic cross-feeding interactions are ubiquitous and can drive important community functions. Engaging in cross-feeding undoubtedly affects the physiology and metabolism of individual species involved. However, the nature in which an individual's physiology is influenced by cross-feeding and the importance of those physiological changes for the mutualism have received little attention. We previously developed a genetically tractable coculture to study bacterial mutualisms. The coculture consists of fermentative *Escherichia coli* and phototrophic *Rhodopseudomonas palustris*. In this coculture, *E. coli* anaerobically ferments sugars into excreted organic acids as a carbon source for *R. palustris*. In return, a genetically-engineered *R. palustris* constitutively converts N_2 into NH_4^+, providing *E. coli* with essential nitrogen. Using RNA-seq and proteomics, we identified transcript and protein levels that differ in each partner when grown in coculture versus monoculture. When in coculture with *R. palustris*, *E. coli* gene-expression changes resembled a nitrogen starvation response under the control of the transcriptional regulator NtrC. By genetically disrupting *E. coli* NtrC, we determined that a nitrogen starvation response is important for a stable coexistence, especially at low *R. palustris* NH_4^+ excretion levels. Destabilization of the nitrogen starvation regulatory network resulted in variable growth trends and in some cases, extinction. Our results highlight that alternative physiological states can be important for survival within cooperative cross-feeding relationships.

Importance

Mutualistic cross-feeding between microbes within multispecies communities is widespread. Studying how mutualistic interactions influence the physiology of each species involved is important for understanding how mutualisms function and persist in both natural and applied settings. Using a bacterial mutualism consisting of *Rhodopseudomonas palustris* and *Escherichia coli* growing cooperatively through bidirectional nutrient exchange, we determined that an *E. coli* nitrogen starvation response is important for maintaining a stable coexistence. The lack of an *E. coli* nitrogen starvation response ultimately destabilized the mutualism and, in some cases, led to community collapse after serial transfers.

Our findings thus inform on the potential necessity of an alternative physiological state for mutualistic coexistence with another species compared to the physiology of species grown in isolation.

Introduction

Within diverse microbial communities, species engage in nutrient cross-feeding with reciprocating partners as a survival strategy (1). In cases where species are not obligate mutualists, transitioning from a free-living lifestyle to one based on cross-feeding can change the physiological state of the cells involved, the extent to which depends on the nature of the cross-feeding relationship. For example, cross-feeding can promote physiological changes that increase virulence (2, 3) or drastically alter cellular metabolism (4), in some cases allowing for lifestyles that are only possible during mutualistic growth with a partner (4–7). Aside from these examples, relatively little is known about how cell physiology is influenced by mutualistic cross-feeding, despite the prevalence of cross-feeding in microbial communities.

Synthetic communities, or cocultures, are ideally suited for studying the physiological responses to cooperative cross-feeding given their tractability (8, 9). We previously developed a bacterial coculture that consists of fermentative *Escherichia coli* and the N_2-fixing photoheterotroph *Rhodopseudomonas palustris* (Fig. 1) (10). In this coculture, *E. coli* anaerobically ferments glucose into organic acids, providing *R. palustris* with essential carbon. In return, a genetically engineered *R. palustris* strain (Nx) constitutively fixes N_2 gas, resulting in NH_4^+ excretion that provides *E. coli* with essential nitrogen. The result is an obligate mutualism that maintains a stable coexistence and reproducible growth trends (10) as long as bidirectional nutrient cross-feeding levels are maintained within a defined range (11, 12).

Here we determined how nutrient cross-feeding between *E. coli* and *R. palustris* Nx alters the physiological state of each partner population. Using RNA-seq and proteomic analyses, we identified genes in both species that were differentially expressed in coculture compared to monoculture, with *E. coli* exhibiting more overall changes in gene expression than *R. palustris* Nx. Specifically, *E. coli* gene-expression patterns resembled that of nitrogen-deprived cells, as many upregulated genes were within the nitrogen-starvation response regulon, controlled by the master transcriptional regulator NtrC. Genetic

disruption of *E. coli ntrC* resulted in variable growth trends at low *R. palustris* NH_4^+ excretion levels and prevented long-term mutualistic coexistence with *R. palustris* across serial transfers. Our results highlight the fact that cross-feeding relationships can stimulate alternative physiological states for at least one of the partners involved and that adjusting cell physiology to these alternative states can be critical for maintaining coexistence.

Results

Engaging in an obligate mutualism alters the physiology of cooperating partners. In our coculture, *E. coli* and *R. palustris* Nx carry out complementary anaerobic metabolic processes whose products serve as essential nutrients for the respective partner. Specifically, *E. coli* ferments glucose into acetate, lactate, and succinate, which serve as carbon sources for *R. palustris* Nx, while other fermentation products such as formate and ethanol accumulate; in return *R. palustris* Nx fixes N_2 and excretes NH_4^+ as the nitrogen source for *E. coli* (Fig. 1). We previously demonstrated that our coculture supports a stable coexistence and exhibits reproducible growth and metabolic trends when started from a wide range of starting species ratios, including single colonies (10). However, we hypothesized that coculture conditions would affect the physiology of each species, particularly *E. coli*, based on the following observations. First, as growth is coupled in our coculture, *E. coli* is forced to grow 4.6-times slower in coculture with *R. palustris* Nx than it does in monoculture with abundant NH_4^+ due to slow NH_4^+ cross-feeding from *R. palustris* Nx (10). In contrast, *R. palustris* Nx grows at a rate in coculture that is comparable to that in monoculture (12), consuming a mixed pool of excreted organic acids from *E. coli*. Second, coculturing pulls *E. coli* fermentation forward due to removal of inhibitory end products. For example, we observed higher yields of formate, an *E. coli* fermentation product that *R. palustris* does not consume, in cocultures compared to *E. coli* monocultures (10).

To determine changes in gene-expression patterns imposed by coculturing, we performed RNA-seq and comparative proteomic analyses (13) on exponential phase cocultures and monocultures of *E. coli* and *R. palustris* Nx. To make direct comparisons, all cultures were grown in the same basal anaerobic

minimal medium, and monocultures were supplemented with the required carbon or nitrogen sources to permit growth for each species. Cocultures and *E. coli* monocultures were provided glucose as a sole carbon source, whereas a mixture of organic acids and bicarbonate was provided to *R. palustris* Nx monocultures, as *R. palustris* does not consume glucose. For a nitrogen source, all cultures were grown under a N_2 headspace, and *E. coli* monocultures were further supplemented with NH_4Cl, as *E. coli* is incapable of using N_2. We identified several differentially expressed genes between monoculture and coculture conditions in both species with more differences observed in *E. coli* compared to *R. palustris* Nx, in agreement with our initial hypothesis (Fig. 2). For *E. coli*, out of 4377 ORFs, 55 were upregulated and 68 were downregulated (Table 1) (log2 value cutoff=2). Out of 4836 ORFs in *R. palustris* Nx, 14 were upregulated and 20 were downregulated (Table 1) (log2 value cutoff=2). We also considered that due to lower *E. coli* abundance in coculture, the apparently larger *E. coli* gene response may be partly due to decreased resolution and thus increased error variance. Reassuringly, many of the genes identified as being differentially expressed by RNA-seq were in agreement with the proteomic results (Table 2). Both RNA-seq and proteomic analyses identified the *E. coli* ammonium transporter AmtB as an important, upregulated gene in coculture, corroborating our previous findings that *E. coli* AmtB activity is important for stable coexistence with *R. palustris* (12). Many *E. coli* genes involved in amino acid and purine biosynthesis were downregulated in coculture (Table 1, Table 2), consistent with the lower observed growth rate. Additionally, many *E. coli* flagellar and chemotaxis proteins were downregulated in coculture (Table 1, Table 2), perhaps suggesting that motility is not important for coculture growth. Alternatively, lower flagellar and chemotaxis transcript levels could be part of a general stress response (14), perhaps associated with nitrogen limitation in cocultures. Whereas many of the differentially expressed *E. coli* genes have been characterized in the literature, the *R. palustris* genes showing the largest differential expression were uncharacterized genes encoding upregulated putative alcohol/aldehyde dehydrogenases and a downregulated putative TonB-dependent receptor/siderophore (Table 1, Table 2). Together, these datasets provide insight on how engaging in obligate cross-feeding changes the lifestyle of each partner.

An *E. coli* nitrogen starvation response is important for mutualistic growth with *R. palustris.* We chose to further examine differential gene expression patterns in *E. coli* as its growth rate and fermentation profile are drastically affected by coculturing, whereas the *R. palustris* Nx growth rate is similar to that in monoculture. We identified several *E. coli* genes and proteins that were upregulated in coculture with *R. palustris* Nx compared to monoculture growth (Table 1, Table 2). We hypothesized that the deletion of highly upregulated *E. coli* genes would negatively affect its growth in coculture. We made deletions in *E. coli* genes that were identified in both RNA-seq and proteome datasets as well as the highest upregulated *E. coli* transcript (*rutA*). We did not examine the effect of deleting *amtB* in this case as we previously determined it to be important for coculture growth (12). These selected *E. coli* genes were all involved in metabolism of alternative nitrogen sources such as D-ala-D-ala dipeptides (*ddpX*, *ddpA*) (15), pyrimidines (*rutA*) (16), amino acids (*argT*) (17), and polyamines (*patA*, *potF*) (18). In monocultures with 15mM NH_4Cl, there were negligible differences in growth or fermentation profiles between WT *E. coli* and any of the single deletion mutants (Fig. S1). These results are consistent with findings by others, as these genes are only important when scavenging alternative nitrogen sources that are not present in our defined medium. We next tested these *E. coli* mutants in coculture with *R. palustris* Nx to determine if these genes were important when NH_4^+ is slowly cross-fed from *R. palustris* Nx. All cocultures using the *E. coli* mutants paired with *R. palustris* Nx exhibited similar growth and population trends to cocultures with WT *E. coli* (Fig. 3). Additionally, there were no significant differences in the growth rates, growth yields, or product yields from cocultures containing the *E. coli* mutants (Fig. S2). These data suggest that none of these highly expressed *E. coli* genes are solely important for coculture growth. While it is possible that synergistic expression of these genes is important for *E. coli's* lifestyle in coculture, the actual nitrogen sources accessed by expression of these genes are absent in the defined medium. Thus, unless *E. coli* gains access to alternative nitrogen sources that we are unaware of in coculture with *R. palustris* Nx, synergistic expression of these genes likely provides little to no benefit.

Even though individual deletions of the *E. coli* genes showing high expression in coculture had no effect on coculture trends, we noted that they were all involved in nitrogen scavenging and fell within the regulon of the transcription factor, NtrC, which controls the nitrogen starvation response (19). During nitrogen limitation, the sensor kinase NtrB phosphorylates the response regulator NtrC (19). Phosphorylated NtrC then binds to DNA and activates expression of ~45 genes (20), including those we tested genetically above and *amtB*, which we previously determined to be important for coculture growth (12). To examine the importance of the *E. coli* nitrogen starvation response in coculture, we deleted *ntrC*. We first checked for any general defects of the resulting ΔNtrC mutant in monoculture with 15 mM NH_4Cl and found that it exhibited similar growth and metabolic trends to WT *E. coli* (Fig. S3). We then paired *E. coli* ΔNtrC with *R. palustris* Nx in coculture. Compared to cocultures using WT *E. coli*, cocultures with *E. coli* ΔNtrC exhibited slower growth rates, longer lag periods (Fig. 4A), and lower final *E. coli* cell densities (Fig. 4D). The long lag phase was less prominent in cocultures inoculated from single colonies (Fig. S4A) compared to cocultures inoculated with a 1% dilution of stationary cocultures (Fig. 4A). This result suggests that starting *E. coli* ΔNtrC cocultures from single colonies stimulated early growth, perhaps by increasing the *E. coli* frequency to be similar to that of *R. palustris* when started with colonies of similar sizes rather than a dilution of stationary cocultures wherein the *E. coli* frequency was low (~0.1%; Fig. 4D). A higher initial *E. coli* frequency might help *E. coli* acquire excreted NH_4^+ before it is taken back up by *R. palustris* cells and thereby promote reciprocal cross-feeding, similar to what we observed previously in cocultures with *E. coli* ΔAmtB mutants that were defective for NH_4^+ uptake (12).

The overall coculture metabolism was also altered when *E. coli* ΔNtrC was paired with *R. palustris* Nx. In cocultures pairing WT *E. coli* with *R. palustris* Nx, glucose is typically fully consumed within 5 days coinciding with the accumulation of formate and ethanol (10). Cocultures pairing *E. coli* ΔNtrC with *R. palustris* Nx differed in this regard, leaving ~40% of the glucose unconsumed after 10 days and exhibiting little to no formate and ethanol accumulation (Fig. S4B). Even despite the lower glucose consumption, the final *R. palustris* cell density of cocultures pairing *R. palustris* Nx with *E. coli* ΔNtrC was similar to those with WT *E. coli*. This unexpectedly high cell density could be explained by

consumption of formate and ethanol by *R. palustris* Nx, though we have never observed consumption of formate by *R. palustris* Nx in monoculture. Alternatively, a lack of formate and/or ethanol production by *E. coli* could explain the high cell density if the fermentation profile were shifted towards organic acids that *R. palustris* normally consumes, namely acetate, lactate and succinate. Together, these data indicate that misregulation of the nitrogen starvation response affected coculture growth and metabolism.

As noted above, the low *E. coli* ΔNtrC population and decreased coculture growth rate when paired with *R. palustris* Nx resembled trends from cocultures that contained *E. coli* ΔAmtB mutants (12). We previously found that the *E. coli* NH_4^+ transporter, AmtB, was required for coexistence with *R. palustris* Nx across serial transfers as the transporter gives *E. coli* a competitive advantage in acquiring the transiently available NH_4^+ before it can be reclaimed by the *R. palustris* population (12). To determine if *E. coli* ΔNtrC was capable of maintaining a stable coexistence in coculture, we inoculated cocultures of *E. coli* ΔNtrC paired with *R. palustris* Nx at equivalent CFUs and performed serial transfers every 10 days. While average final *E. coli* frequencies were consistently between 0.6 – 2.8 % (Fig. 5A), the values became variable over serial transfers, as did coculture growth rates, lag periods, and net changes in both *E. coli* and *R. palustris* cell densities (Fig. 5). This variability was due to 2 of the 4 lineages exhibiting improved coculture growth over successive transfers (Fig. 5B, C), perhaps due to the emergence of compensatory mutations, while the other two lineages showed declining growth trends (Fig. 5D, E). Indeed, by transfers 5 and 6 there was little to no coculture growth in the slower-growing lineages (Fig 4D, E). The heterogeneity in growth trends through serial transfers of cocultures with *E. coli* ΔNtrC is in stark contrast to the stability of cocultures with WT *E. coli*, which we have serially transferred over 100 times with no extinction events (McKinlay, unpublished data). The nitrogen starvation response thus appears to be important for long-term survival of the mutualism.

Increased NH_4^+ cross-feeding levels can compensate for the absence of a nitrogen starvation response. The NtrC regulon is critical during periods of nitrogen starvation, activating a wide variety of genes that are important for scavenging diverse nitrogen sources (20). We hypothesized that higher *R.*

palustris NH_4^+ cross-feeding levels could mitigate the poor growth of *E. coli* ΔNtrC in coculture by making the nitrogen starvation response less important for survival. Previously, we engineered an *R. palustris* Nx strain that excretes 3-times more NH_4^+ by deleting *R. palustris* NH_4^+ transporters encoded by *amtB1* and *amtB2* (NxΔAmtB) (10). N_2-fixing bacteria use AmtB to reacquire NH_4^+ that leaks outside the cell, and ΔAmtB mutants thus accumulate NH_4^+ into the supernatant (10, 12, 21). In agreement with our hypothesis, cocultures with *R. palustris* NxΔAmtB exhibited similar growth trends regardless of the *E. coli* strain used (Fig. 4B, D). As *R. palustris* NxΔAmtB excretes more NH_4^+ than *R. palustris* Nx, it was previously shown to result in faster WT *E. coli* growth and subsequent fermentation rates in coculture, ultimately leading to the accumulation of consumable organic acids (Fig. S4B) and acidification of the medium, inhibiting *R. palustris* growth (10). Cocultures pairing *R. palustris* NxΔAmtB and *E. coli* ΔNtrC similarly exhibited growth (Fig. 4B,D), and fermentation profile trends (Fig. S4B) that were indistinguishable from cocultures pairing *R. palustris* NxΔAmtB with WT *E. coli*. These similar trends indicate that high *R. palustris* NH_4^+ excretion can eliminate the trends observed when the *E. coli* nitrogen starvation response is compromised due to a ΔNtrC mutation.

One possibility for why high NH_4^+ cross-feeding levels eliminate the need for *E. coli ntrC* is that the free NH_4^+ levels might be sufficiently high enough to prevent activation of the *E. coli* NtrC regulon. However, comparative RNA-seq and proteomic analyses revealed that the same *E. coli* genes within the NtrC regulon that were highly upregulated in cocultures pairing WT *E. coli* with *R. palustris* Nx were also upregulated in cocultures with *R. palustris* NxΔAmtB (Table 1, Table 2). Thus, even though the *E. coli* nitrogen-starvation response is activated when cocultured with *R. palustris* NxΔAmtB, this response is likely dispensable if there is sufficiently high NH_4^+ cross-feeding.

E. coli NtrC is required for adequate AmtB expression to access cross-fed NH_4^+ in coculture. While a high level of *R. palustris* NH_4^+ excretion can compensate for an improper *E. coli* nitrogen-starvation response, less NH_4^+ excretion could potentially exaggerate problems emerging from the absence of NtrC. We previously constructed an *R. palustris* ΔAmtB strain that excreted 1/3rd of the NH_4^+ than *R. palustris*

Nx in monoculture and which could not coexist in coculture with *E. coli* ΔAmtB (12). The reason for this lack of coexistence was due to *R. palustris* ΔAmtB outcompeting *E. coli* ΔAmtB for the lower level of transiently available NH_4^+, thus limiting *E. coli* growth and thereby the reciprocal supply of fermentation products to *R. palustris* (12). Expression of *E. coli amtB* is thus important in coculture in order to maintain coexistence. Indeed, RNA-seq and proteomic analyses revealed that *E. coli* AmtB transcript and protein levels were upregulated in all cocultures pairing WT *E. coli* with any of the three *R. palustris* strains (Nx, NxΔAmtB, ΔAmtB) (Table 1, Table 2). We thus wondered whether *E. coli* ΔNtrC would coexist with the low NH_4^+-excreting strain *R. palustris* ΔAmtB in coculture, as *E. coli amtB* expression is transcriptionally activated by NtrC. Consistent with our previous findings, *R. palustris* ΔAmtB supported a high relative WT *E. coli* population in coculture (Fig. 4D) (12). When cocultured with WT *E. coli*, *R. palustris* ΔAmtB responds to NH_4^+ loss to *E. coli* by upregulating nitrogenase activity since it has a wild-type copy of NifA (12). As a result, *R. palustris* ΔAmtB cross-feeds enough NH_4^+ to stimulate a high WT *E. coli* frequency and subsequent accumulation of consumable organic acids, similar to cocultures with *R. palustris* NxΔAmtB (Fig 3D, Fig. S4B) (12). In contrast, when we paired *E. coli* ΔNtrC with *R. palustris* ΔAmtB, little to no coculture growth was observed (Fig. 4C), similar to previous observations in cocultures pairing *E. coli* ΔAmtB with *R. palustris* ΔAmtB (12). Cocultures inoculated with single colonies of each species in this pairing grew to low cell densities (Fig. S4A), and cocultures inoculated from these cocultures resulted in little to no growth, even after prolonged incubation (Fig. 4C).

As AmtB is under the control of NtrC (20), we hypothesized that cocultures pairing *E. coli* ΔNtrC with *R. palustris* ΔAmtB resulted in insufficient *E. coli amtB* expression, leading to a decreased ability to capture NH_4^+, which *R. palustris* will reaquire if given the chance (12). We thus predicted that increased expression of *amtB* in *E. coli* ΔNtrC would result in increased net growth of both species, as *E. coli* ΔNtrC would be more competitive for essential NH_4^+ and be able to grow and produce more organic acids for *R. palustris* ΔAmtB. To test this prediction, we obtained a plasmid harboring an IPTG-inducible copy of *amtB* (p*amtB*) for use in *E. coli* ΔNtrC. AmtB is typically tightly regulated and only expressed when

NH_4^+ concentrations are below 20 μM, as cells acquire sufficient NH_4^+ through passive diffusion of NH_3 across the membrane at higher concentrations (22). Additionally, excessive NH_4^+ uptake through AmtB transporters that exceeds the rate of assimilation can result in a futile cycle, as excess NH_3 inevitably diffuses outside the cell (19). We first tested the effect of p*amtB* in WT *E. coli* monocultures with 15 mM NH_4Cl. Induction with 1 mM IPTG prevented growth whereas 0.1 mM IPTG permitted growth albeit at a decreased growth rate (Fig. S5). We thus decided to use 0.1 mM IPTG to induce *amtB* expression in all cocultures described below. In cocultures pairing *E. coli* ΔNtrC p*amtB* with *R. palustris* ΔAmtB, more growth was observed than in cocultures with *E. coli* ΔNtrC harboring an empty vector (pEV) (Fig. 6A). In cocultures with *E. coli* ΔNtrC pEV, the *R. palustris* ΔAmtB cell density increased whereas the *E. coli* cell density did not (Fig. 6B). The *R. palustris* growth was likely due to growth-independent cross-feeding of fermentation products from *E. coli* maintenance metabolism, a phenomenon we described previously (11). In contrast, cell densities of both species increased in cocultures pairing *R. palustris* ΔAmtB with *E. coli* ΔNtrC p*amtB* (Fig. 6C), in agreement with our hypothesis that poor *E. coli amtB* expression contributed to the lack of growth in this coculture pairing. While *E. coli amtB* expression in this coculture pairing was sufficient to restore growth of both species, there are likely other genes within the NtrC regulon that contribute to *E. coli* growth in coculture. For example, the *E. coli* NtrC-regulated serine/threonine kinase yeaG has been shown to play a role in survival during nitrogen starvation by promoting metabolic heterogeneity (23). Indeed, *E. coli* yeaG and its associated protein of unknown function yeaH are both highly upregulated in coculture (Table 1). Thus, while we cannot rule out that other genes within the *E. coli ntrC* regulon are not important for coculture growth, the necessity of NtrC to upregulate *amtB* is clearly important.

Discussion

In this study, we found that reciprocal nutrient cross-feeding between *E. coli* and *R. palustris* resulted in significant changes in gene expression in both species compared to monocultures. Based on the RNA-seq and proteomic analyses, we determined that *E. coli* alters its physiology to adopt a nitrogen-starved state

277 in response to low NH_4^+ cross-feeding levels from *R. palustris*. We subsequently determined that this
278 nitrogen-starved state is important for coexistence as genetic elimination of the master transcriptional
279 regulator, NtrC, resulted in variable population outcomes. Mutualistic nutrient cross-feeding has also been
280 shown to change the lifestyle of interacting partners in other systems. In natural communities, nutrient
281 cross-feeding can alter gene-expression patterns to adapt each species to a syntrophic lifestyle (24–27). In
282 some cases, the lifestyles exhibited within a mutualism might not even be possible during growth in
283 isolation. For example, in synthetic communities that pair the sulfate-reducer *Desulfovibiro vulgaris* with
284 the methanogen *Methanococcus maripaludis*, the methanogen consumes H_2, which maintains low partial
285 pressures that permit the sulfate reducer to adopt a fermentative lifestyle that would otherwise be
286 thermodynamically infeasible (5). Similarly, in an experimental *Geobacter* coculture, direct electron
287 transfer from *Geobacter metallireducens* to *Geobacter sulfurreducens* makes ethanol fermentation by *G.*
288 *metallireducens* thermodynamically possible (7).

289 Similar to our mutualistic system, the mutualism between *D. vulgaris* and *M. maripaludis*
290 represents a facultative mutualism, at least in the short term prior to evolutionary erosion of independent
291 lifestyles (28). For mutualistic relationships to persist between partners that are conditionally capable of a
292 free-living lifestyle, the relationship must exhibit resilience, or the ability to recover its function after a
293 disturbance (29). One important resilience factor is the activation of regulatory networks that allow for
294 microbes to quickly respond to environmental perturbations. Whereas flexible gene expression is useful
295 for an individual microbe's survival, excessive flexibility can sometimes lead to community collapse
296 between mutualists in a fluctuating environment (30, 31). In the coculture of *D. vulgaris* and *M.*
297 *maripaludis*, alternating between coculture and monoculture conditions, which require different metabolic
298 lifestyles, resulted in community collapse (30, 31). Surprisingly, community collapse could be avoided by
299 mutations that disrupted the *D. vulgaris* regulatory response needed to adapt cells for optimal growth rates
300 in monoculture (30). Disruption of this regulatory response resulted in a heterogeneous *D. vulgaris*
301 population, ensuring that a subpopulation would be primed for immediate mutualistic growth upon
302 transition between growth conditions (31). In our system, the *E. coli* nitrogen starvation regulatory

network was specifically activated by coculturing with *R. palustris* and was important for coculture stability. It is currently unclear if transitioning *E. coli* between monoculture and coculture conditions would result in similar community collapse or whether the NtrC-regulated network would adjust rapidly enough to meet the demands of each condition.

Nutrient starvation and other stress responses are widely conserved in diverse microbes and are primarily regarded as necessary for an individual's survival in nutrient-limited environments (32–35). Many microbial communities are composed of primarily slow-growing or even non-growing subpopulations (36–38). However, lack of microbial growth in these communities does not imply cessation of cross-feeding, as bacteria often carry out growth-independent maintenance processes at slow rates (39), and such activities can be coupled to cross-feeding (11). Our findings suggest that nutrient starvation and perhaps other stress responses can help stabilize microbial cross-feeding interactions, especially at low nutrient cross-feeding levels. The extent to which specific starvation or stress responses are active in diverse mutualistic relationships remains unclear, yet likely depends on the environmental context. Together our results highlight the important role that alternate physiological states, including stress responses, can play in establishing and maintaining mutualistic cross-feeding relationships.

Materials and Methods

Strains and growth conditions. Strains, plasmids, and primers are listed in Table S1. All *R. palustris* strains contained *ΔuppE* and *ΔhupS* mutations to facilitate accurate colony forming unit (CFU) measurements by preventing cell aggregation (40) and to prevent H_2 uptake, respectively. *E. coli* was cultivated on Luria-Burtani (LB) agar and *R. palustris* on defined mineral (PM) (41) agar with 10 mM succinate. $(NH_4)_2SO_4$ was omitted from PM agar for determining *R. palustris* CFUs. Monocultures and cocultures were grown in 10 mL of defined M9-derived coculture medium (MDC) (10) in 27-mL anaerobic test tubes under 100% N_2 as described (10). For harvesting RNA and protein, 100-mL cultures were grown in 260-mL serum vials. In both cases, MDC was supplemented with cation solution (1 % v/v; 100 mM $MgSO_4$ and 10 mM $CaCl_2$) and glucose (25 mM), unless indicated otherwise. *R. palustris*

329 monocultures were further supplemented with 15 mM sodium bicarbonate, 7.8 mM sodium acetate, 8.7
330 mM disodium succinate, 1.5 mM sodium lactate, 0.3 mM sodium formate, and 6.7mM ethanol. *E. coli*
331 monocultures were further supplemented with 2.5 mM NH_4Cl. Kanamycin was added to a final
332 concentration of 30 μg/ml for *E. coli* where appropriate. Chloramphenicol was added to a final
333 concentration of 5 μg/ml for both *R. palustris* and *E. coli* where appropriate. All cultures were grown at
334 30°C laying horizontally under a 60 W incandescent bulb with shaking at 150 rpm. Starter cocultures
335 were inoculated with 200 μL MDC containing a suspension of a single colony of each species. Test
336 cocultures and serial transfers were inoculated using a 1% dilution from starter cocultures. For
337 experiments requiring a starting species ratio of 1:1, *E. coli* and *R. palustris* starter monocultures were
338 grown to equivalent cell densities, and inoculated at equal volumes.

339 **Generation of *E. coli* mutants.** P1 transduction (42) was used to introduce deletions from Keio
340 collection strains into MG1655. The genotype of kanamycin-resistant colonies was confirmed by PCR
341 and sequencing.

342 **Analytical procedures.** Cell density was assayed by optical density at 660 nm (OD_{660}) using a Genesys
343 20 visible spectrophotometer (Thermo-Fisher, Waltham, MA, USA). Growth curve readings were taken
344 in culture tubes without sampling (i.e., tube OD_{660}). Specific growth rates were determined using readings
345 between 0.1-1.0 OD_{660} where there is linear correlation between cell density and OD_{660}. Final OD_{660}
346 measurements were taken in cuvettes and samples were diluted into the linear range as necessary.
347 Glucose, organic acids, formate and ethanol were quantified using a Shimadzu high-performance liquid
348 chromatograph (HPLC) as described (43).

349 **Sample collection for transcriptomics and proteomics.** Monocultures and cocultures were grown in
350 100-mL volumes to late exponential phase and chilled in an ice-water bath. A 1-mL sample was collected
351 for protein quantification using a Pierce BCA Protein Assay Kit as per the manufacturer's protocol. A 5-
352 ml sample was removed for RNA extraction and 90 ml was used for proteomic analysis. All samples were
353 centrifuged at 4°C, supernatants discarded, and cell pellets frozen in liquid N_2 and stored at -80°C.

RNA-seq. Total RNA was isolated from cell pellets using the RNeasy kit (Qiagen, Valencia, CA, USA) as per the manufacturer's protocol. In order to calculate baseline expression levels, RNA sequencing reads resulting from monoculture were mapped to their corresponding reference genome (*E. coli* str. K-12 substr. MG1655 (44), NCBI RefSeq: NC_000913.3; *R. palustris* CGA0009 (45), NCBI RefSeq: NC_005296.1) using the Tuxedo protocol for RNA expression analysis (46) (Workflow deposited at https://github.com/behrimg/Task3/RNASeq). Specifically, split-reads were aligned to the reference genome with Tophat2 (v.2.1.0) (47) and Bowtie2 (v.2.1.0) (48). Following mapping, transcripts were assembled with cufflinks (v.2.2.0) (49), and differential expression was identified with the cufflinks tool, cuffdiff (v.2.2.0). To assure that crossmapping of homologous sequencing reads would not complicate expression analysis from the co-culture experiments, monoculture reads were additionally mapped as described to the opposing genome. As all potential crossmapping was confined to residual rRNA reads, these regions were excluded from the analysis and the co-culture RNA-seq reads where analyzed by mapping the sequenced reads to both reference genomes with no further correction.

Preparation of protein samples for MS. Cell pellets were resuspended in 1 mL total protein buffer (TPB; 20mM HEPES-NaOH pH7.4, 150mM NaCl, 2mM EDTA, 0.2mM DTT, 1:100 PMSF, 1:100 protease inhibitors cocktail IV) and sonicated at 20% intensity (7 seconds on, 7 seconds off) for 5 min in an ice bath. Then 1/10 volume of 20% SDS was added. Samples were vortexed, boiled for 5 min, and immediately placed on ice. Debris was cleared by centrifuging for 30 s at 10,000 x g at 4°C and the supernatant was collected. Protein content of different lysates was analyzed by Coomassie staining following SDS-PAGE and sample aliquots containing 200 µg protein were subjected to chloroform:methanol protein extraction as described (50).

Analysis by LC-MS/MS. Mass spectrometry was performed at the Mass Spectrometry and Proteomics Research Laboratory (MSPRL), FAS Division of Science, at Harvard University. Samples were individually labeled with tandem mass tag (TMT) 10-plex reagents according to the manufacturer's protocol (ThermoFisher Scientific) and mixed. The mixed sample was dried in a speedvac and re-diluted with Buffer A (0.1 % formic acid in water) for injection for HPLC runs. The sample was submitted for a

single liquid chromatography coupled to tandem mass spectrometry (LC-MS/MS) experiment which was performed on a LTQ Orbitrap Elite (ThermoFisher Scientific) equipped with Waters (Milford, MA) NanoAcquity HPLC pump Peptides were separated onto a 100 µm inner diameter microcapillary trapping column packed first with approximately 5 cm of C18 Reprosil resin (5 µm, 100 Å, Dr. Maisch GmbH, Germany) followed by analytical column ~20 cm of Reprosil resin (1.8 µm, 200 Å, Dr. Maisch GmbH, Germany). Separation was achieved through applying a gradient from 5–27% ACN in 0.1% formic acid over 90 min at 200 nl min−1. Electrospray ionization was enabled through applying a voltage of 1.8 kV using a home-made electrode junction at the end of the microcapillary column and sprayed from fused silica pico tips (New Objective, MA). The LTQ Orbitrap Elite was operated in data-dependent mode for the mass spectrometry methods. The mass spectrometry survey scan was performed in the Orbitrap in the range of 395 –1,800 m/z at a resolution of 6×10^4, followed by the selection of the twenty most intense ions (TOP20) for CID-MS2 fragmentation in the ion trap using a precursor isolation width window of 2 m/z, AGC setting of 10,000, and a maximum ion accumulation of 200 ms. Singly charged ion species were not subjected to CID fragmentation. Normalized collision energy was set to 35 V and an activation time of 10 ms. Ions in a 10 ppm m/z window around ions selected for MS2 were excluded from further selection for fragmentation for 60 s. The same TOP20 ions were subjected to HCD MS2 event in Orbitrap part of the instrument. The fragment ion isolation width was set to 0.7 m/z, AGC was set to 50,000, the maximum ion time was 200 ms, normalized collision energy was set to 27V and an activation time of 1 ms for each HCD MS2 scan.

Mass spectrometry data analysis. Raw data were submitted for analysis in MaxQuant 1.5.6.5 (13). Assignment of MS/MS spectra was performed by searching the data against a protein sequence database including all entries from the *E. coli* MG1655 proteome (51), the *R. palustris* CGA009 proteome (45), and other known contaminants such as human keratins and common lab contaminants. MaxQuant searches were performed using a 20 ppm precursor ion tolerance with a requirement that each peptide had N termini consistent with trypsin protease cleavage, allowing up to two missed cleavage sites. 10-plex TMT tags on peptide amino termini and lysine residues were set as static modifications while methionine

406 oxidation and deamidation of asparagine and glutamine residues were set as variable modifications. MS2
407 spectra were assigned with a false discovery rate (FDR) of 1% at the protein level by target-decoy
408 database search. Per-peptide reporter ion intensities were exported from MaxQuant (evidence.txt). Only
409 peptides with a parent ion fraction greater than or equal to 0.5 were used for subsequent analysis (6063 of
410 9987 peptides). Intensities were calculated as the sum of peptide intensities. Ratios between conditions
411 were computed at the peptide level, and the protein ratio was computed as the mean of peptide ratios. All
412 ratios were normalized by dividing by the median value for proteins from the same species. Ratio
413 significance for coculture conditions at an FDR of 1% was computed by determining the ratio *r* at which
414 99% of genes have ratio less than *r* when comparing biological replicate monocultures.

415 **Expression of *E. coli amtB* in coculture.** The ASKA collection (52) plasmid harboring an IPTG-
416 inducible copy of *amtB* (pCA24N *amtB*) was purified from strain JW0441-AM and introduced by
417 electroporation into WT *E. coli* and *E. coli* ΔNtrC. Cocultures were inoculated with either single colonies
418 of each species or at a 1:1 starting species ratio, as indicated in the figure legends. IPTG and 5 μg/ml
419 chloramphenicol were supplemented to cocultures to induce *E. coli amtB* expression in cocultures and
420 maintain the plasmid, respectively.

421

422 **Acknowledgments**

423 We thank B. A. Budnik and R. A. Robins (Harvard MSPRL) for assistance with mass spectrometry.
424 We thank P. L. Foster for providing the Keio and ASKA *E. coli* collections. This work was supported in
425 part by the U.S. Department of Energy, Office of Science, Office of Biological and Environmental
426 Research under Award Number DE-SC0008131 to JBM, by the U.S. Army Research Office, grant
427 W911NF-14-1-0411 to ML, DAD, and JBM, by a National Institutes of Health National Service Award
428 F32GM123703 to MGB, and by the Indiana University College of Arts and Sciences.

429

430 **References**

431 1. Seth EC, Taga ME. 2014. Nutrient cross-feeding in the microbial world. Front. Microbiol. 5:1–6.

2. Hammer ND, Cassat JE, Noto MJ, Lojek LJ, Chadha AD, Schmitz JE, Creech CB, Skaar EP. 2014. Inter-and intraspecies metabolite exchange promotes virulence of antibiotic-resistant *Staphylococcus aureus*. Cell Host Microbe 16:531–537.

3. Ramsey MM, Rumbaugh KP, Whiteley M. 2011. Metabolite cross-feeding enhances virulence in a model polymicrobial infection. PLoS Pathog. 7:1–8.

4. Iannotti EL, Kafkewit D, Wolin MJ, Bryant MP. 1973. Glucose fermentation products of *Ruminococcus albus* grown in continuous culture with *Vibrio succinogenes* - Changes caused by interspecies transfer of H_2. J. Bacteriol. 114:1231–1240.

5. Stolyar S, Van Dien S, Hillesland KL, Pinel N, Lie TJ, Leigh JA, Stahl DA. 2007. Metabolic modeling of a mutualistic microbial community. Mol. Syst. Biol. 3:92.

6. Walker CB, Redding-Johanson AM, Baidoo EE, Rajeev L, He Z, Hendrickson EL, Joachimiak MP, Stolyar S, Arkin AP, Leigh JA, Zhou J, Keasling JD, Mukhopadhyay A, Stahl DA. 2012. Functional responses of methanogenic archaea to syntrophic growth. ISME J. 6:2045–2055.

7. Summers ZM, Fogarty HE, Leang C, Franks AE, Malvankar NS, Lovley DR. 2010. Direct exchange of electrons within aggregates of an evolved syntrophic coculture of anaerobic bacteria. Science 330:1413–5.

8. Widder S, Allen RJ, Pfeiffer T, Curtis TP, Wiuf C, Sloan WT, Cordero OX, Brown SP, Momeni B, Shou W, Kettle H, Flint HJ, Haas AF, Laroche B, Kreft J. 2016. Challenges in microbial ecology: building predictive understanding of community function and dynamics. ISME J. 10:2557–2568.

9. Lindemann SR, Bernstein HC, Song H-S, Fredrickson JK, Fields MW, Shou W, Johnson DR, Beliaev AS. 2016. Engineering microbial consortia for controllable outputs. ISME J. 10:2077–2084.

10. LaSarre B, McCully AL, Lennon JT, McKinlay JB. 2017. Microbial mutualism dynamics governed by dose-dependent toxicity of cross-fed nutrients. ISME J. 11:337–348.

11. McCully AL, LaSarre B, McKinlay JB. 2017. Growth-independent cross-feeding modifies boundaries for coexistence in a bacterial mutualism. Environ. Microbiol. 19:3538-3550.

12. McCully AL, LaSarre B, McKinlay JB. 2017. Recipient-biased competition for an intracellularly generated cross-fed nutrient is required for coexistence of microbial mutualists. mBio 8:e01620-17.

13. Cox J, Mann M. 2008. MaxQuant enables high peptide identification rates, individualized p.p.b.-range mass accuracies and proteome-wide protein quantification. Nat. Biotechnol. 26:1367–1372.

14. Jozefczuk S, Klie S, Catchpole G, Szymanski J, Cuadros-Inostroza A, Steinhauser D, Selbig J, Willmitzer L. 2010. Metabolomic and transcriptomic stress response of *Escherichia coli*. Mol. Syst. Biol. 6:1–16.

15. Lessard IAD, Pratt SD, McCaffertyl DG, Bussiere DE, Hutchins C, Wanner BL, Katz L, Walsh CT. 1998. Homologs of the vancomycin resistance D-Ala-D-Ala dipeptidase VanX in *Streptomyces toyocaensis*, *Escherichia coli* and *Synechocystis* : attributes of catalytic efficiency, stereoselectivity and regulation with implications for function. Chem. Biol. 5:489-504.

16. Kim KS, Pelton JG, Inwood WB, Andersen U, Kustu S, Wemmer DE. 2010. The Rut pathway for pyrimidine degradation: Novel chemistry and toxicity problems. J. Bacteriol. 192:4089–4102.

17. Caldara M, Charlier D, Cunin R. 2006. The arginine regulon of *Escherichia coli*: Whole-system transcriptome analysis discovers new genes and provides an integrated view of arginine regulation. Microbiology 152:3343–3354.

18. Kashiwagi K, Pistocchi R, Shibuya S, Sugiyama S, Morikawa K, Igarashi K. 1996. Spermidine-preferential uptake system in *Escherichia coli*. J. Biol. Chem. 271:12205–12208.

19. van Heeswijk WC, Westerhoff H V., Boogerd FC. 2013. Nitrogen assimilation in *Escherichia coli*: Putting molecular data into a systems perspective. Microbiol. Mol. Biol. Rev. 77:628–695.

20. Zimmer DP, Soupene E, Lee HL, Wendisch VF, Khodursky AB, Peter BJ, Bender RA, Kustu S. 2000. Nitrogen regulatory protein C-controlled genes of *Escherichia coli*: scavenging as a defense against nitrogen limitation. Proc. Natl. Acad. Sci. U. S. A. 97:14674–14679.

21. Barney BM, Eberhart LJ, Ohlert JM, Knutson CM, Plunkett MH. 2015. Gene deletions resulting in increased nitrogen release by *Azotobacter vinelandii*: Application of a novel nitrogen biosensor. Appl. Environ. Microbiol. 81:4316–4328.

22. Kim M, Zhang Z, Okano H, Yan D, Groisman A, Hwa T. 2012. Need-based activation of ammonium uptake in *Escherichia coli*. Mol. Syst. Biol. 8:1–10.

23. Figueira R, Brown DR, Ferreira D, Eldridge MJG, Burchell L, Pan Z, Helaine S, Wigneshweraraj S.

2015. Adaptation to sustained nitrogen starvation by *Escherichia coli* requires the eukaryote-like serine/threonine kinase YeaG. Sci. Rep. 5:1–14.

24. Rosenthal AZ, Matson EG, Eldar A, Leadbetter JR. 2011. RNA-seq reveals cooperative metabolic interactions between two termite-gut spirochete species in co-culture. ISME J. 5:1133–1142.

25. Filkins LM, Graber JA., Olson DG, Dolben EL, Lynd LR, Bhuju S, Toole AO, O'Toole GA. 2015. Coculture of *Staphylococcus aureus* with *Pseudomonas aeruginosa* drives *S. aureus* towards fermentative metabolism and reduced viability in a cystic fibrosis model. J. Bacteriol. 197:2252-2264.

26. Men Y, Feil H, VerBerkmoes NC, Shah MB, Johnson DR, Lee PKH, West KA, Zinder SH, Andersen GL, Alvarez-Cohen L. 2012. Sustainable syntrophic growth of *Dehalococcoides ethenogenes* strain 195 with *Desulfovibrio vulgaris* Hildenborough and *Methanobacterium congolense*: global transcriptomic and proteomic analyses. ISME J. 6:410–421.

27. Giannone RJ, Huber H, Karpinets T, Heimerl T, Küper U, Rachel R, Keller M, Hettich RL, Podar M. 2011. Proteomic characterization of cellular and molecular processes that enable the *Nanoarchaeum equitans-Ignicoccus hospitalis* relationship. PLoS One 6:e22942.

28. Hillesland KL, Lim S, Flowers JJ, Turkarslan S, Pinel N, Zane GM, Elliott N, Qin Y, Wu L, Baliga NS, Zhou J, Wall JD, Stahl DA. 2014. Erosion of functional independence early in the evolution of a microbial mutualism. Proc. Natl. Acad. Sci. 111:14822–14827.

29. Song HS, Renslow RS, Fredrickson JK, Lindemann SR. 2015. Integrating ecological and engineering concepts of resilience in microbial communities. Front. Microbiol. 6:1–7.

30. Turkarslan S, Raman A V, Thompson AW, Arens CE, Gillespie MA, von Netzer F, Hillesland KL, Stolyar S, López García de Lomana A, Reiss DJ, Gorman‐Lewis D, Zane GM, Ranish JA, Wall JD, Stahl DA, Baliga NS. 2017. Mechanism for microbial population collapse in a fluctuating resource environment. Mol. Syst. Biol. 13:919.

31. Thompson AW, Turkarslan S, Arens CE, López García de Lomana A, Raman A V., Stahl DA, Baliga NS. 2017. Robustness of a model microbial community emerges from population structure among single cells of a clonal population. Environ. Microbiol. 19:3059–3069.

32. Kjelleberg S, Albertson N, Flardh K, Holmquist L, Jouper-Jaan A, Marouga R, Ostling J, Svenblad B,

Weichart D. 1993. How do non-differentiating bacteria adapt to starvation? Antonie Van Leeuwenhoek 63:333–341.

33. Shimizu K. 2013. Regulation systems of bacteria such as *Escherichia coli* in response to nutrient limitation and environmental stresses. Metabolites 4:1–35.

34. Barbara S, Resources N, Collins F. 2007. Microbial stress-response physiology and its implications 88:1386–1394.

35. Roszak DB, Colwell RR. 1987. Survival strategies of bacteria in the natural environment. Microbiol. Rev. 51:365–379.

36. Jørgensen BB, Marshall IPG. 2016. Slow microbial life in the seabed. Ann. Rev. Mar. Sci. 8:311–332.

37. Bergkessel M, Basta DW, Newman DK. 2016. The physiology of growth arrest: uniting molecular and environmental microbiology. Nat. Rev. Microbiol. 14:549–562.

38. Lennon JT, Jones SE. 2011. Microbial seed banks: The ecological and evolutionary implications of dormancy. Nat. Rev. Microbiol. 9:119–130.

39. Wanner U, Egli T. 1990. Dynamics of microbial growth and cell composition in batch culture. FEMS Microbiol. Rev. 6:19–43.

40. Fritts RK, LaSarre B, Stoner AM, Posto AL, McKinlay JB. 2017. A *Rhizobiales*-specific unipolar polysaccharide adhesin contributes to *Rhodopseudomonas palustris* biofilm formation across diverse photoheterotrophic conditions. Appl. Environ. Microbiol. 83: e03035-16.

41. Kim M-K, Harwood CS. 1991. Regulation of benzoate-CoA ligase in *Rhodopseudomonas palustris*. FEMS Microbiol. Lett. 83:199–203.

42. Thomason LC, Costantino N, Court DL. 2007. *E. coli* genome manipulation by P1 transduction. Curr. Protoc. Mol. Biol. 1.17.1-1.17.8.

43. McKinlay JB, Zeikus JG, Vieille C. 2005. Insights into *Actinobacillus succinogenes* fermentative metabolism in a chemically defined growth medium. Appl Env. Microbiol 71:6651–6656.

44. Hayashi K, Morooka N, Yamamoto Y, Fujita K, Isono K, Choi S, Ohtsubo E, Baba T, Wanner BL, Mori H, Horiuchi T. 2006. Highly accurate genome sequences of *Escherichia coli* K-12 strains MG1655 and W3110. Mol. Syst. Biol. 2:2006.0007.

45. Larimer FW, Chain P, Hauser L, Lamerdin J, Malfatti S, Do L, Land ML, Pelletier D a, Beatty JT, Lang AS, Tabita FR, Gibson JL, Hanson TE, Bobst C, Torres JLTY, Peres C, Harrison FH, Gibson J, Harwood CS. 2004. Complete genome sequence of the metabolically versatile photosynthetic bacterium *Rhodopseudomonas palustris*. Nat. Biotechnol. 22:55–61.

46. Trapnell C, Roberts A, Goff L, Pertea G, Kim D, Kelley DR, Pimentel H, Salzberg SL, Rinn JL, Pachter L. 2012. Differential gene and transcript expression analysis of RNA-seq experiments with TopHat and Cufflinks. Nat. Protoc. 7:562–578.

47. Kim D, Pertea G, Trapnell C, Pimentel H, Kelley R, Salzberg SL. 2013. TopHat2: accurate alignment of transcriptomes in the presence of insertions, deletions and gene fusions. Genome Biol. 14:R36.

48. Langmead B, Salzberg SL. 2012. Fast gapped-read alignment with Bowtie 2. Nat. Methods 9:357–9.

49. Trapnell C, Williams BA, Pertea G, Mortazavi A, Kwan G, van Baren MJ, Salzberg SL, Wold BJ, Pachter L. 2010. Transcript assembly and quantification by RNA-Seq reveals unannotated transcripts and isoform switching during cell differentiation. Nat. Biotechnol. 28:511–515.

50. Wallace EWJ, Kear-Scott JL, Pilipenko EV., Schwartz MH, Laskowski PR, Rojek AE, Katanski CD, Riback JA, Dion MF, Franks AM, Airoldi EM, Pan T, Budnik BA, Drummond DA. 2015. Reversible, specific, active aggregates of endogenous proteins assemble upon heat stress. Cell 162:1286–1298.

51. The UniProt Consortium. 2017. UniProt: The universal protein knowledgebase. Nucleic Acids Res. 45:D158–D169.

52. Kitagawa M, Ara T, Arifuzzaman M, Ioka-Nakamichi T, Inamoto E, Toyonaga H, Mori H. 2005. Complete set of ORF clones of *Escherichia coli* ASKA library (A complete set of *E. coli* K-12 ORF archive): unique resources for biological research. DNA Res. 12:291–299.

53. Blattner F, Plunkett G I, Bloch C, Perna N, Burland V, Riley M, Collado-Vides J, Glasner J, Rode C, Mayhew G, Gregor J, Davis N, Kirkpatrick H, Goeden M, Rose D, Mau B, Shao Y. 1997. The complete genome sequence of *Escherichia coli* K-12. Science. 277:1453–1462.

54. Baba T, Ara T, Hasegawa M, Takai Y, Okumura Y, Baba M, Datsenko KA, Tomita M, Wanner BL, Mori H. 2006. Construction of *Escherichia coli* K-12 in-frame, single-gene knockout mutants: the Keio collection. Mol. Syst. Biol. 2:2006.0008.

Figure Legends

Table 1. Selected differentially expressed transcripts in cocultures of *E. coli* and *R. palustris* compared to monocultures

			***Rp* Nx + *Ec* WT**		***Rp* NxΔAmtB + *Ec* WT**		***Rp* ΔAmtB + *Ec* WT**	
Species	**Gene symbol**	**Gene description**	**Fold change [c]**	**FDR adjusted P-value**	**Fold change**	**FDR adjusted P-value**	**Fold change**	**FDR adjusted P-value**
E. coli	rutA [b]	Pyrimidine monooxygenase	114.5 ± 0.0	0.09	108.0 ± 0.0	0.09	118.0 ± 0.1	0.09
	rutC [b]	Aminoacrylate peracid reductase	60.7 ± 0.1	0.01	58.0 ± 0.1	0.01	60.9 ± 0.1	0.01
	ddpX [ab]	D-ala dipeptidase	58.3 ± 0.1	0.01	59.9 ± 0.1	0.01	50.1 ± 0.0	0.01
	rutD [b]	Aminoacrylate hydrolase	56.9 ± 0.0	0.01	52.9 ± 0.1	0.01	56.6 ± 0.1	0.01
	rutE [b]	Malonic semialdehyde	48.8 ± 0.1	0.01	44.4 ± 0.1	0.01	48.2 ± 0.1	0.01
	rutF [b]	FMN reductase	45.2 ± 0.1	0.01	40.3 ± 0.1	0.01	45.5 ± 0.1	0.01
	patA [ab]	Putrescine aminotransferase	36.3 ± 0.1	0.01	33.6 ± 0.1	0.01	34.4 ± 0.0	0.01
	argT [ab]	Lysine/arginine/ornithine binding protein	35.1 ± 0.3	0.01	38.9 ± 0.3	0.01	35.3 ± 0.3	0.01
	rutG [b]	FMN reductase	28.5 ± 0.0	0.01	26.9 ± 0.0	0.01	29.0 ± 0.1	0.01
	ddpA [ab]	Probably dipeptide binding periplasmid protein	23.7 ± 0.0	0.01	26.8 ± 0.0	0.01	21.0 ± 0.0	0.01
	amtB [ab]	Ammonium transporter	21.3 ± 0.2	0.02	25.0 ± 0.2	0.01	24.1 ± 0.2	0.01
	yeaG [b]	Eukaryotic-like serine/threonine kinase	13.6 ± 0.0	0.08	15.2 ± 0.0	0.04	14.5 ± 0.1	0.06
	yeaH [b]	Unknown	12.8 ± 0.0	0.06	14.2 ± 0.1	0.05	14.0 ± 0.1	0.06
	metE	Methionine biosynthesis	-16.2 ± 0.1	0.03	23.6 ± 0.6	0.03	22.8 ± 0.5	0.02
	fimF	Fimbriae regulatory protein	-16.3 ± 0.0	0.01	18.4 ± 0.0	0.01	20.3 ± 0.1	0.01
	tar	Methyl-accepting chemotaxis protein II	-16.3 ± 0.2	0.01	15.8 ± 0.2	0.02	15.4 ± 0.2	0.01
	purL [a]	Purine biosynthesis	-16.8 ± 0.0	0.03	20.4 ± 0.1	0.02	18.8 ± 0.0	0.02
	flgD	Flagellar basal body rod modification protein	-17.1 ± 0.1	0.02	16.9 ± 0.0	0.01	17.4 ± 0.1	0.01
	ilvL [a]	Isoleucine biosynthesis	-17.4 ± 0.7	0.02	14.9 ± 0.4	0.02	14.2 ± 0.5	0.02
	pgaB	Glucosamine deacetylase	-17.9 ± 0.0	0.02	18.8 ± 0.0	0.03	17.3 ± 0.0	0.04
	ilvC [a]	Isoleucine biosynthesis	-18.0 ± 0.2	0.03	17.1 ± 0.2	0.04	17.6 ± 0.2	0.03
	metK	Methionine biosynthesis	-19.2 ± 0.1	0.03	17.5 ± 0.1	0.03	17.4 ± 0.1	0.04
	tap	Methyl-accepting chemotaxis protein IV	-19.7 ± 0.3	0.01	22.0 ± 0.2	0.01	22.1 ± 0.2	0.01
	flgC	Flagellar basal body	-20.1 ± 0.1	0.05				
	purK [a]	Purine biosynthesis	-20.7 ± 0.1	0.03	25.1 ± 0.1	0.01	21.02 ± 0.05	0.03
	metA	Methionine biosynthesis	-21.0 ± 0.1	0.02	20.6 ± 0.1	0.02	20.8 ± 0.2	0.02
	ilvG [a]	Isoleucine biosynthesis	-22.1 ± 0.1	0.01	19.3 ± 0.1	0.03	22.14 ± 0.07	0.01

	metF	Methionine biosynthesis	-23.3 ± 0.1	0.01	22.5 ± 0.1	0.01	17.62 ± 0.38	0.03
	nadB	Aspartate oxidase	-24.3 ± 0.0	0.08	29.1 ± 0.1	0.05	23.74 ± 0.01	0.07
R. palustris	RPA1206 [a]	Aldehyde dehydrogenase	36.0 ± 0.9	0.02			62.4 ± 0.4	0.01
	RPA1205 [a]	Putative alcohol dehydrogenase	32.8 ± 0.5	0.02			28.6 ± 0.4	0.01
	RPA0538	Putative porin	31.6 ± 2.3	0.03				
	RPA1009 [a]	Possible cytochrome P450	10.4 ± 0.8	0.03				
	RPA3101 [a]	Unknown	9.4 ± 0.3	0.03			10.3 ± 0.3	0.04
	RPA4045 [a]	Putative aa ABC transport	8.8 ± 0.4	0.02				
	RPA3100	Unknown	7.8 ± 0.2	0.02				
	RPA1010	Beta-lactamase-like	7.7 ± 0.4	0.04				
	RPA4020 [a]	Putative aa ABC transport permease	7.7 ± 0.2	0.02				
	RPA1204	Unknown	7.4 ± 0.1	0.02			7.4 ± 0.1	0.03
	RPA2376	Unknown	-6.9 ± 0.1	0.04	15.4 ± 0.2	0.04	9.0 ± 0.2	0.03
	RPA2142	Putative fatty acid CoA ligase	-7.3 ± 0.1	0.03				
	RPA2377	Unknown	-8.4 ± 0.2	0.02	16.4 ± 0.6	0.05	7.3 ± 0.1	0.02
	RPA2379	Probable acetyltransferase	-8.5 ± 0.3	0.02				
	RPA2390	Possible Rhizobactin siderophore biosynthesis	-9.6 ± 0.2	0.06	22.8 ± 0.2	0.05	16.8 ± 0.5	0.03
	RPA1260 [a]	Universal stress protein	-10.5 ± 0.0	0.02			7.2 ± 0.0	0.07
	RPA2380	Possible tonB dep iron siderophore	-11.4 ± 0.6	0.03	17.1 ± 0.1	0.06	18.4 ± 0.2	0.01
	RPA1259	Putative cation-transporting P-type ATPase	-11.6 ± 0.4	0.02			10.6 ± 0.0	0.06
	RPA2378 [a]	Putative TonB-dep receptor	-13.1 ± 0.1	0.03	24.1 ± 0.3	0.06	17.5 ± 0.3	0.02

Genes shown in table were directly or indirectly mentioned in the text. For a full list of differentially-expressed genes, see Supplementary Data.

[a] Genes were also identified as differentially expressed proteins in coculture (Table 2).

[b] Gene is transcriptionally activated by *E. coli* NtrC during nitrogen limitation.

[c] Fold-change values represent mean ± SD. Positive values indicate gene was upregulated in coculture. Negative values indicate gene was downregulated in coculture. Initial cutoff was set to a $\log_2$ value of 2 in at least 2 of 3 biological replicates. For a complete list of all differentially regulated transcripts, refer to supplementary data. Differential expression was determined with the Cufflinks tool cuffdiff (v.2.2.0) (46)

576 **Table 2. Selected differentially expressed proteins in cocultures of *E. coli* and *R. palustris* compared to monocultures**

			Rp Nx + Ec WT	Rp NxΔAmtB + Ec WT	Rp ΔAmtB + Ec WT
Species	**Gene Symbol**	**Gene Description**	**Normalized Relative Protein Intensity [c]**	**Normalized Relative Protein Intensity [d]**	**Normalized Relative Protein Intensity [d]**
E. coli	argT [ab]	Lysine/arginine/ornithine binding protein	10.9	11.1	10.3
	ddpA [ab]	D-ala dipeptide permease	5.8	7.2	6.8
	gss	Bifunctional glutathionylspermidine synthetase/amidase	4.5	4.7	4.0
	tktB	Transketolase	4.1	5.5	3.8
	potF [ab]	Putrescine-binding periplasmic protein	3.8	4.2	4.1
	modA	Molybdate-binding periplasmic protein	3.8	4.0	4.9
	gabD [ab]	Succinate-semialdehyde dehydrogenase	3.7	4.8	3.5
	dapB	4-hydroxy-tetrahydrodipicolinate reductase	3.6	2.8	2.7
	talA	Transaldolase A	3.6	4.2	4.4
	amtB [ab]	NH4+ Transporter	3.5	3.5	3.5
	asnS	Asparagine biosynthesis	-2.1	-1.9	-1.9
	serA	Serine biosynthesis	-2.1	-2.5	-2.3
	secE	Protein translocase subunit	-2.1	-1.8	-2.3
	glf	LPS biosynthesis	-2.1	-1.9	-1.9
	yjiM	Putative dehydratase	-2.2	-1.9	-1.8
	sstT	Serine/threonine transporter	-2.2	-2.4	-2.4
	rmlA1	Carbohydrate biosynthesis	-2.3	-2.1	-2.4
	ompF	Outer membrane protein	-2.3	-2.3	-2.6
	ribE	Riboflavin biosynthesis	-2.3	-1.7	-1.9
	secY	Protein translocase subunit	-2.6	-2.0	-2.0
	glyA	Glycine biosynthesis	-3.2	-3.0	-3.4
	purE [a]	Purine biosynthesis	-3.3	-3.6	-3.5
	yqjI	Transcriptional regulator	-3.6	-3.0	-3.4
	asnA	Aspartate-ammonia ligase	-6.4	-3.8	-3.7
R. palustris	RPA1206 [a]	Aldehyde dehydrogenase	10.0		3.3
	RPA1205 [a]	Putative alcohol dehydrogenase	7.8	1.2	3.9
	RPA3101 [a]	Unknown	7.1	1.5	2.6
	RPA3093	ABC transporter urea/short-chain binding protein	4.8	1.6	3.4
	RPA3297	ABC transporter urea/short-chain binding protein	4.7	1.5	3.2
	RPA4019	Putative aa ABC transporter system substrate-binding protein	3.9	1.4	2.5
	RPA4045 [a]	Putative aa ABC transport	3.3	1.4	2.1
	RPA1009 [a]	Possible cytochrome P450	3.2	1.3	2.1
	RPA1748	Putative branched-chain amino acid transport system	-2.1	-1.4	-2.5

	substrate-binding protein			
RPA2378 [a]	Putative tonB-dependent receptor protein	-2.1	-1.2	-1.1
RPA2124	TonB dependent iron siderophore receptor	-2.3	-1.5	-1.7
RPA1260 [a]	Universal stress protein	-2.5	-1.5	-1.8
RPA2050	Unknown	-2.7	-1.6	-2.6
RPA3669	Putative ABC transporter periplasmic solute-binding protein precursor	-2.8	-1.1	-1.3
RPA2120	Periplasmic binding protein	-6.0	-1.6	-1.7

Proteins shown in table were directly or indirectly mentioned in the text. For a full list of differentially-expressed proteins, see Supplementary Data.

[a] Genes were also identified as differentially expressed transcripts in coculture (Table 1)

[b] Gene is transcriptionally activated by *E. coli* NtrC

Values represent mean normalized relative protein intensity for either two [c] or one [d] biological replicate. Positive values indicate gene was upregulated in coculture. Negative values indicate gene was downregulated in coculture.

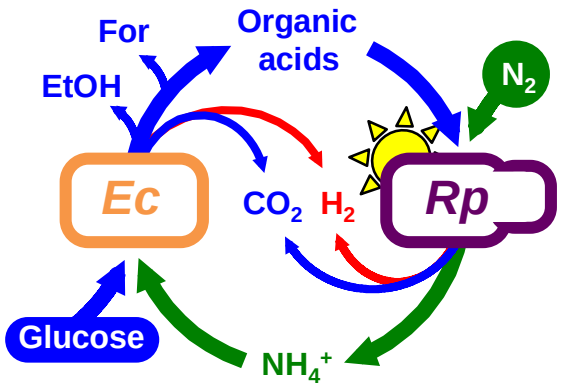

FIG 1. Bidirectional cross-feeding of carbon and nitrogen in an anaerobic bacterial mutualism between fermentative *Escherichia coli (Ec)* and phototrophic *Rhodopseudomonas palustris (Rp)*. *E. coli* anaerobically ferments glucose into excreted organic acids that *R. palustris* Nx consumes (acetate, lactate and succinate) and other products that *R. palustris* Nx does not consume (formate (For) and ethanol (EtOH)). In return, *R. palustris* Nx constitutively fixes N_2 gas and excretes NH_4^+, supplying *E. coli* with essential nitrogen. *R. palustris* Nx grows photoheterotrophically wherein organic compounds are used for carbon and electrons, and light is used for energy.

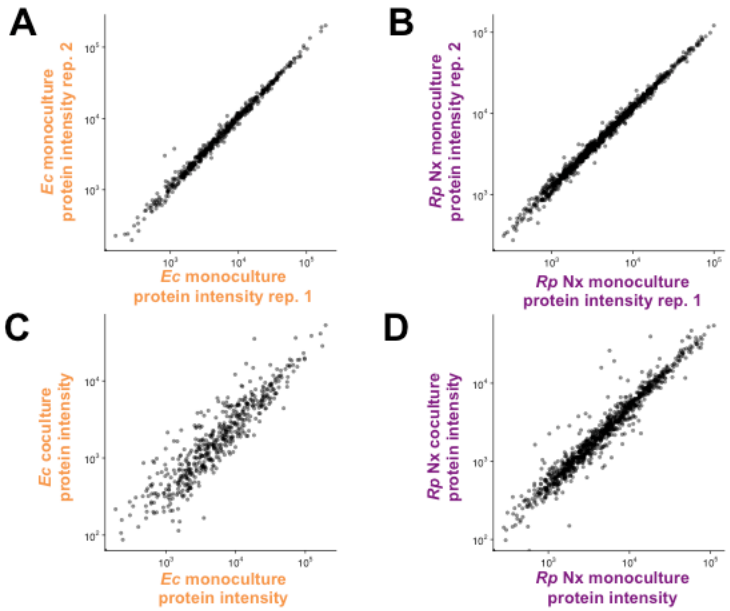

FIG 2. Coculture conditions result in altered protein expression patterns in both species, with more differences in WT *E. coli* compared to *R. palustris* Nx. Protein expression (estimated by LC-MS/MS intensity) of wild-type *E. coli* (left, **A**,**C**) and *R. palustris* Nx (right, **B**, **D**) comparing protein expression patterns between monoculture biological replicates (rep. 1 versus rep. 2, **A**, **B**) and monoculture (average over monoculture replicates) versus coculture (**C**, **D**).

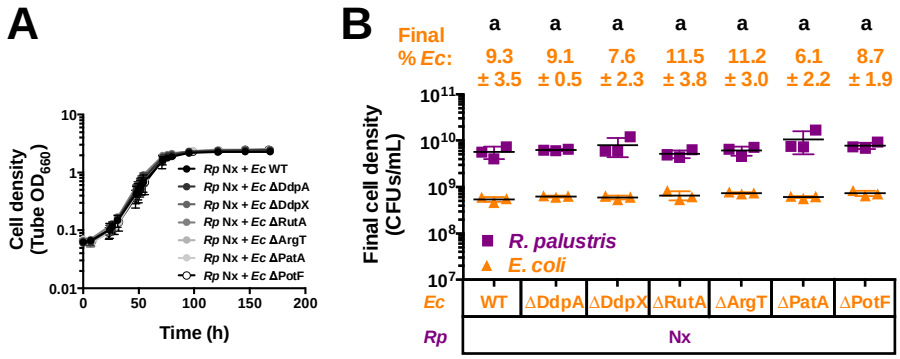

FIG 3. Single deletions of upregulated *E. coli* genes do not impair mutualistic growth with *R. palustris* Nx. Growth curves (**A**) and final cell densities (**B**) from cocultures pairing *E. coli* (*Ec*) mutants with deletions in highly upregulated genes with *R. palustris* (*Rp*) Nx. Final cell densities (**B**) were taken at the final time point in (**A**). Cocultures were started with a 1% inoculum of stationary starter cocultures grown from single colonies. Error bars indicate SD, n=3. Different letters indicate statistical differences, $p < 0.05$, determined by one-way ANOVA with Tukey's multiple comparisons posttest.

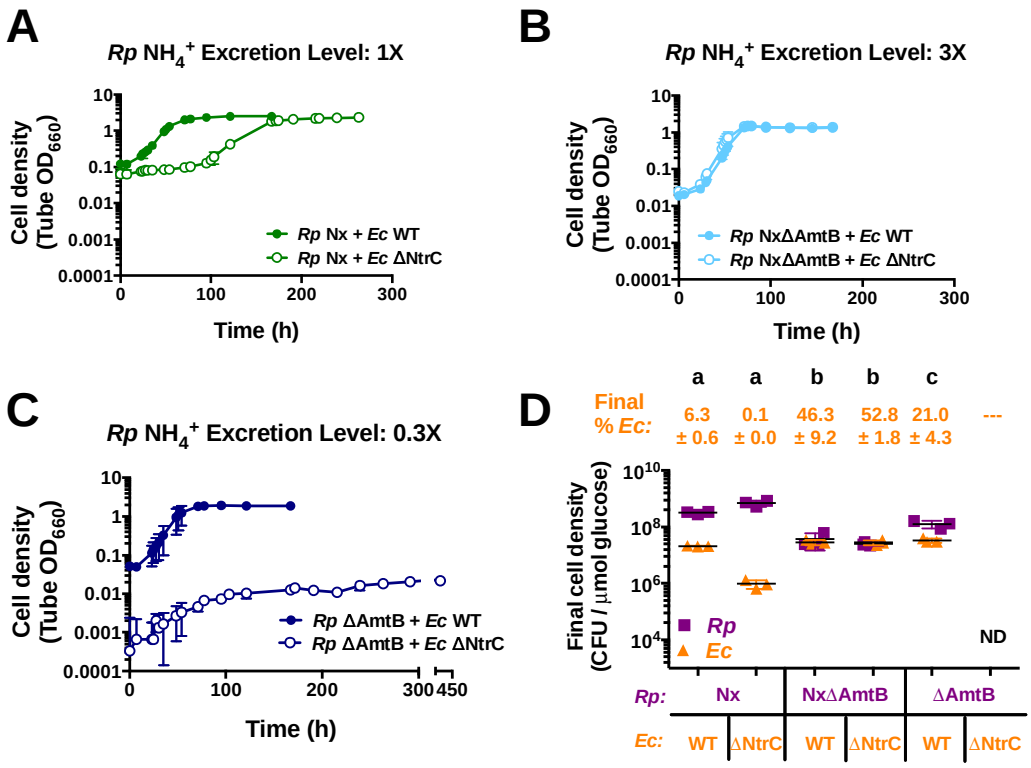

FIG 4. *R. palustris* NH_4^+ excretion level affects growth and population trends in cocultures with *E. coli* NtrC. Growth curves (**A**, **B**, **C**) and final cell densities normalized to glucose consumption (**D**) from cocultures pairing WT *E. coli* (*Ec*) (filled circles) or ΔNtrC (open circles) with *R. palustris* (*Rp*) strains with different NH_4^+ excretion levels. Final cell densities (**D**) were taken at the final time point in the respective growth curve (**A**, **B**, **C**), except for cocultures pairing *R. palustris* ΔAmtB with *E. coli* ΔNtrC which were sampled at 260 h. Cell densities were normalized to glucose consumed to account for incomplete glucose consumption in cocultures containing *E. coli* ΔNtrC. Cocultures were started with a 1% inoculum of stationary starter cocultures grown from single colonies. Error bars indicate SD, n=3. Different letters indicate statistical differences, $p < 0.05$, determined by one-way ANOVA with Tukey's multiple comparisons posttest. ND, not determined.

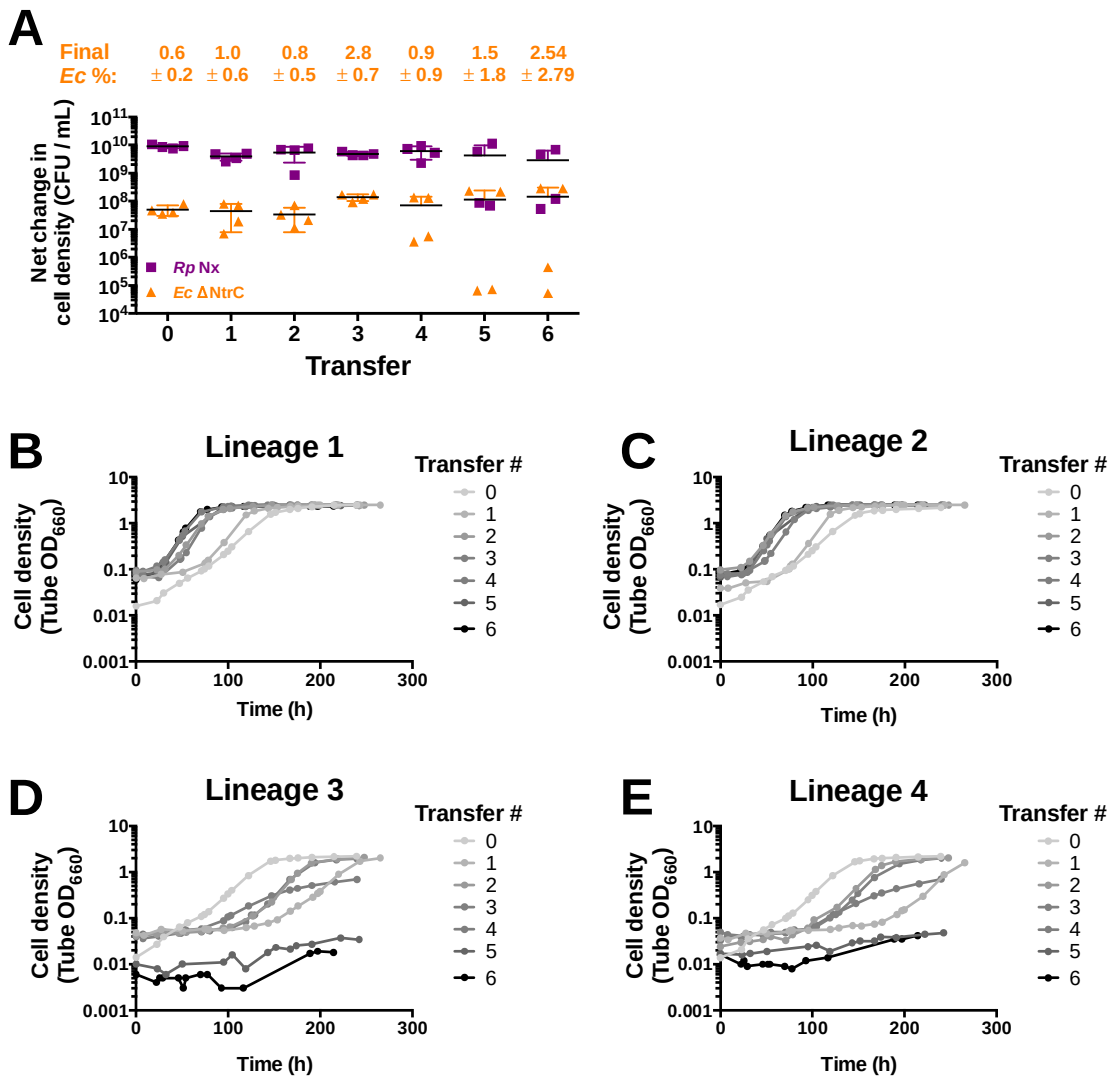

FIG 5. Lack of *E. coli* NtrC results in variable coculture growth trends across serial transfers. Net changes in cell densities (**A**) and replicate growth curves (**B-E**) of cocultures pairing *E. coli* (*Ec*) ΔNtrC with *R. palustris* (*Rp*) Nx across serial transfers. Cocultures were initially inoculated (Transfer 0) at a 1:1 starting species ratios based on CFUs/mL from *R. palustris* and *E. coli* monocultures. A 1% inoculum was used for each serial transfer. Transfers were performed every 10 d. Error bars indicate SD, n=4.

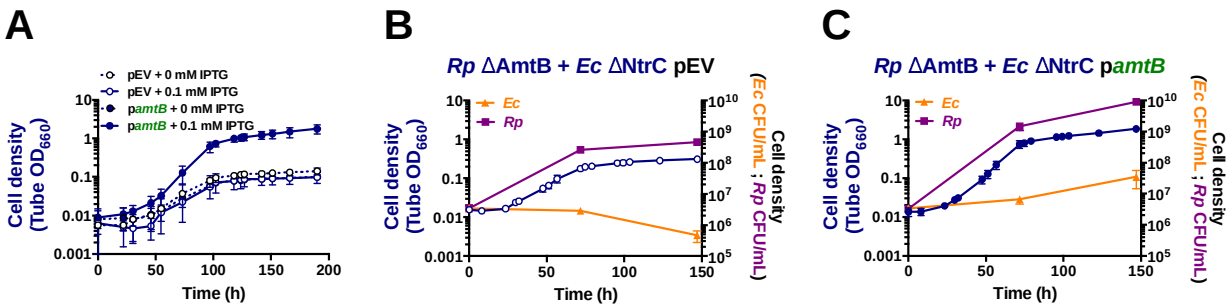

625

626 **FIG 6. Ectopic expression of *amtB* in *E. coli* ΔNtrC permits mutualistic growth with *R. palustris***
627 **ΔAmtB.** Growth curves (**A-C**) and cell densities for each species (**B**, **C**) from cocultures pairing *R.*
628 *palustris* (*Rp*) ΔAmtB with *E. coli* (*Ec*) ΔNtrC harboring a plasmid encoding an IPTG-inducible copy of
629 *amtB* (p*amtB*, filled circles) or an empty vector (pEV, open circles). To maintain plasmids, all cocultures
630 were supplemented with 5 μg/ml chloramphenicol, which is otherwise lethal to *E. coli* but not to *R.*
631 *palustris* (Fig. S6). Cocultures were inoculated with a single colony of each species (**A**) or at a 1:1
632 starting species ratio based on equivalent CFUs/mL from starter *R. palustris* and *E. coli* monocultures (**B**,
633 **C**). 0.1 mM IPTG was added to the cocultures at the initial time point. Error bars indicate SD, n=3.

Supplemental

Table S1. Strains and plasmids

Strain or plasmid	Description or Sequence (5'-3'); Designation in this study	Source or Purpose
***R. palustris* strains**		
CGA009	Wild-type strain; spontaneous Cm^R derivative of CGA001	(45)
CGA4005	CGA009 Δ*hupS* Δ*uppE nifA**; Nx	(10)
CGA4021	CGA4005 Δ*amtB1* Δ*amtB2*; NxΔAmtB	(10)
CGA4026	CGA009 Δ*hupS* Δ*uppE* Δ*amtB1* Δ*amtB2*; ΔAmtB	(12)
***E. coli* strains**		
MG1655	Wild-type K12 strain; WT	(53)
K-12 JW1483	Keio collection Δ*ddpX::Km*	(54)
K-12 JW5240	Keio collection Δ*ddpA::Km*	(54)
K-12 JW0997	Keio collection Δ*rutA::Km*	(54)
K-12 JW2307	Keio collection Δ*argT::Km*	(54)
K-12 JW5510	Keio collection Δ*patA::Km*	(54)
K-12 JW0838	Keio collection Δ*potF::Km*	(54)
K-12 JW3840	Keio collection Δ*ntrC::Km*	(54)
K-12 pCA24N (pASKA)	ASKA collection pCA24N	(52)
MG1655 pCA24N -GFP	ASKA collection pCA24N with gfp removed using NotI digest	This study
K-12 JW0441-AM pASKAamtB	ASKA collection pCA24N-N-His-amtB (gfp minus)	(52)
MG1655ΔDdpX	MG1655 Δ*ddpX::Km*; ΔDdpX	This study
MG1655ΔDdpA	MG1655 Δ*ddpA::Km*; ΔDdpA	This study
MG1655ΔRutA	MG1655 Δ*rutA::Km*; ΔRutA	This study
MG1655ΔArgT	MG1655 Δ*argT::Km*; ΔArgT	This study
MG1655ΔPatA	MG1655 Δ*patA::Km*; ΔPatA	This study
MG1655ΔPotF	MG1655 Δ*potF::Km*; ΔPotF	This study
MG1655ΔNtrC	MG1655 Δ*ntrC::Km*; ΔNtrC	This study
MG1655 pEV	MG1655 pCA24N; WT pEV	This study
MG1655ΔNtrC pEC	MG1655 Δ*ntrC::Km* pCA24N; ΔNtrC pEV	This study
MG1655 p*amtB*	MG1655 pCA24N-N-His-*amtB*+; WT p*amtB*	This study
MG1655ΔNtrC p*amtB*	MG1655 Δ*ntrC::Km* pCA24N-N-His-*amtB*+; ΔNtrC p*amtB*	This study
Plasmids		
pCA24N	Cm^R; ASKA collection empty vector with IPTG-inducible promoter	(52)
pCA24N-*amtB*+	Cm^R; ASKA collection vector with IPTG-inducible promoter in front of N-terminal His-tagged *amtB* gene	(52)
Primers		

ALM47	cggaaagcgcagcaatttttgt	*ddpX* upstream flanking region (*E. coli*)
ALM48	gagcaatgtgggacgaaacg	*ddpX* downstream flanking region (*E. coli*)
ALM45	atatcccctggcacacagc	*ddpA* upstream flanking region (*E. coli*)
ALM46	ccagcagcgttggcgtaaaata	*ddpX* downstream flanking region (*E. coli*)
ALM51	ccgctttgcaaacaagcc	*rutA* upstream flanking region (*E. coli*)
ALM52	atcagcgcactttgctgc	*rutA* downstream flanking region (*E. coli*)
ALM49	gcaaacacacaacacaatacacaac	*argT* upstream flanking region (*E. coli*)
ALM50	ccatcaggtacagcttccca	*argT* downstream flanking region (*E. coli*)
ALM53	tgaaagcgtgctgttaacgc	*patA* upstream flanking region (*E. coli*)
ALM54	atcccgattttcgcgatcg	*patA* downstream flanking region (*E. coli*)
ALM55	ctggccgggagaaagttct	*potF* upstream flanking region (*E. coli*)
ALM56	ttacgggttttcgcctgc	*potF* downstream flanking region (*E. coli*)
MO 7	caatctttacacacaagctgtgaatc	*ntrC* upstream flanking region (*E. coli*)
MO 8	cctgcctatcaggaaataaagg	*ntrC* downstream flanking region (*E. coli*)
pCA24N.for	gataacaatttcacacagaattcattaaagag	ASKA pCA24N upstream into IPTG-inducible promoter upstream of cloned gene
pCA24N.rev	cccattaacatcaccatctaattcaac	ASKA pCA24N downstream into IPTG-inducible promoter upstream of cloned gene

636

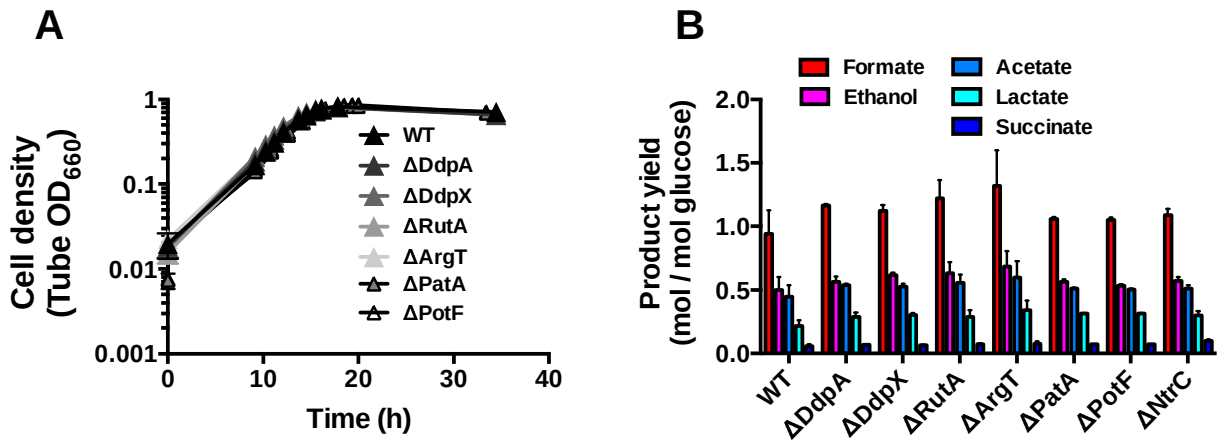

637

638 **FIG S1. Single deletions of *E. coli* genes that were upregulated in coculture no effect in monoculture**

639 **with 15 mM NH_4^+.** Growth curves (**A**) and product yields (**B**) from *E. coli* monocultures grown with 15

640 mM NH_4Cl. Product yields were taken in stationary phase. Error bars indicate SD, n=3.

641

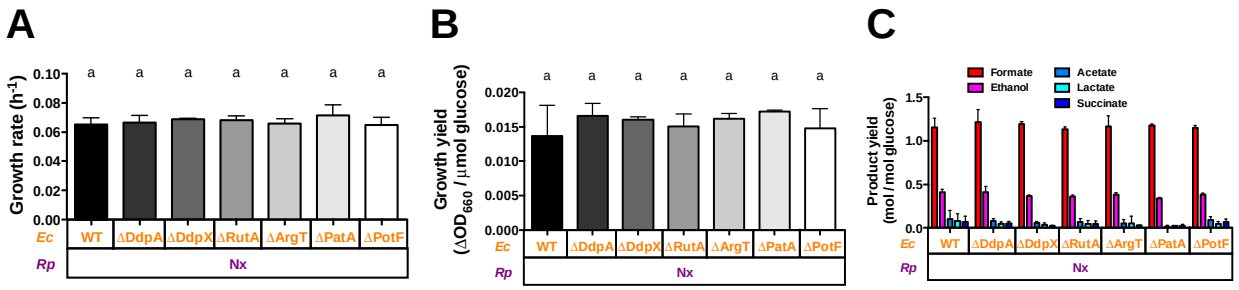

642

643 **FIG S2. Additional trends from cocultures pairing *R. palustris* Nx with *E. coli* single deletions**

644 **mutants.** Growth rates (**A**), growth yields (**B**), and product yields (**C**) after a one-week culturing period

645 from cocultures pairing *E. coli* mutants with deletions in highly upregulated genes with *R. palustris* Nx.

646 Growth and product yields were taken at the final time point indicated in Fig. 3A. Cocultures were started

647 with a 1% inoculum of stationary starter cocultures grown from single colonies. Error bars indicate SD,

648 n=3. Different letters indicate statistical differences, $p < 0.05$, determined by one-way ANOVA with

649 Tukey's multiple comparisons posttest.

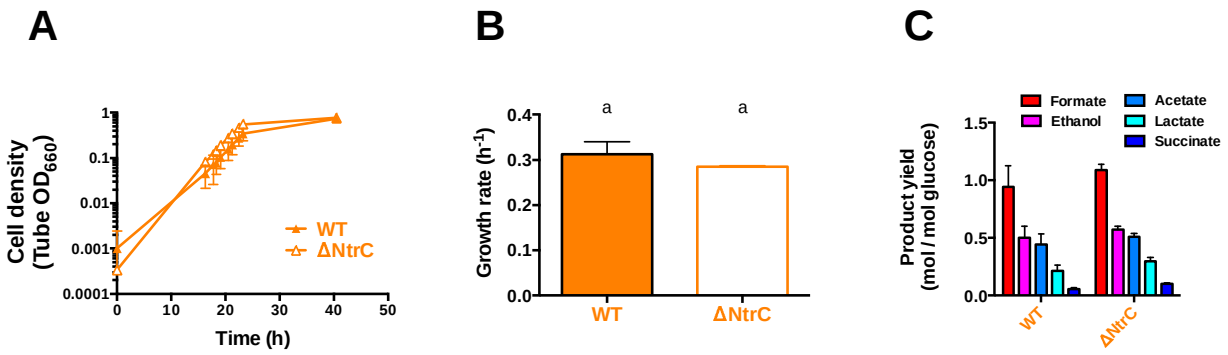

650

651 **FIG S3. *E. coli* ΔNtrC growth and metabolic trends are similar to those of WT *E. coli* in**

652 **monoculture with 15 mM NH_4^+.** Growth curves (**A**), growth rate (**B**) and product yields (**C**) from WT *E.*

653 *coli* (filled) or ΔNtrC (open) monocultures grown with 15 mM NH_4Cl. Product yields were taken in

654 stationary phase. Error bars indicate SD, n=3.

655

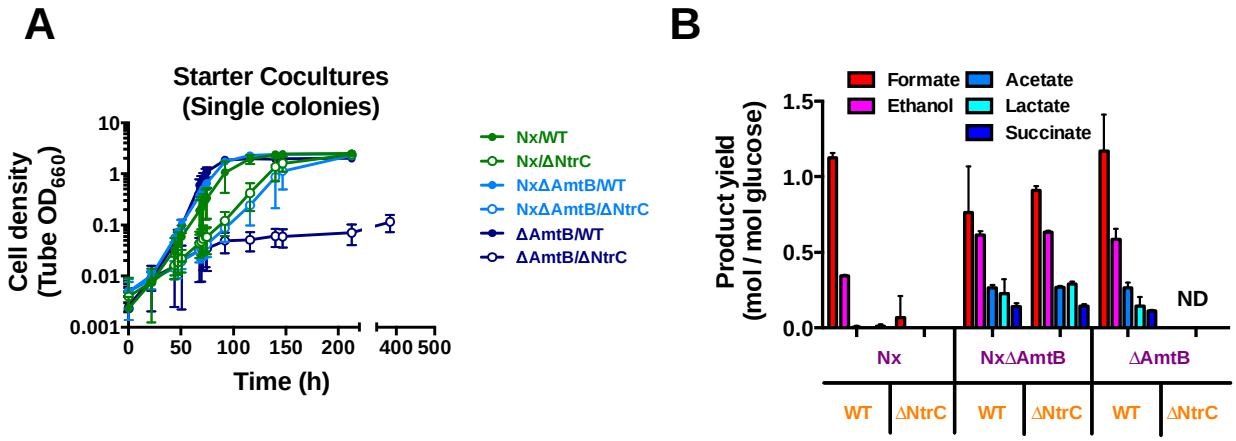

656

657 **FIG S4. Additional trends from cocultures of *E. coli* ΔNtrC paired with different *R. palustris***

658 **partners.** Growth curves of starter cocultures inoculated with single colonies of each species (**A**) and

659 product yields from test cocultures (**B**). Product yields (**B**) were taken at the final time point indicated in

660 the respective growth curve in Fig. 4. Test cocultures were started with a 1% inoculum of stationary

661 starter cocultures. Error bars indicate SD, n=3. ND, not determined.

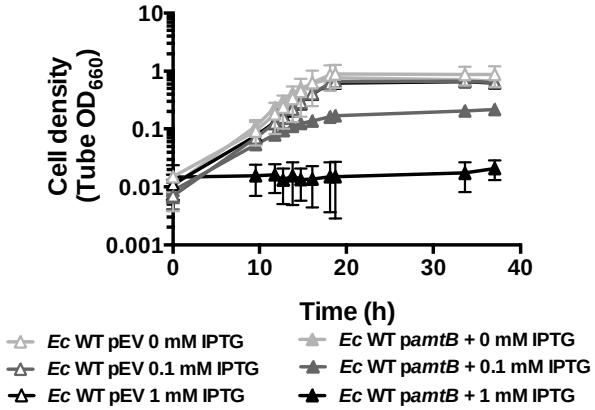

FIG S5. Increased *amtB* expression is harmful to *E. coli* in monocultures with 15 mM NH_4^+. Growth curves of WT *E. coli* monocultures harboring a plasmid encoding an IPTG-inducible copy of *amtB* (p*amtB*, filled) or empty vector (pEV, open) and grown at different IPTG concentrations. All monocultures were supplemented with 15 mM NH_4Cl and 5 μg/ml chloramphenicol to maintain the plasmid. Cultures were inoculated with a 1% inoculum from stationary monocultures grown in 0 mM IPTG. After inoculation, IPTG was added to the indicated final concentration. Error bars indicate SD, n=3. ND, not determined.

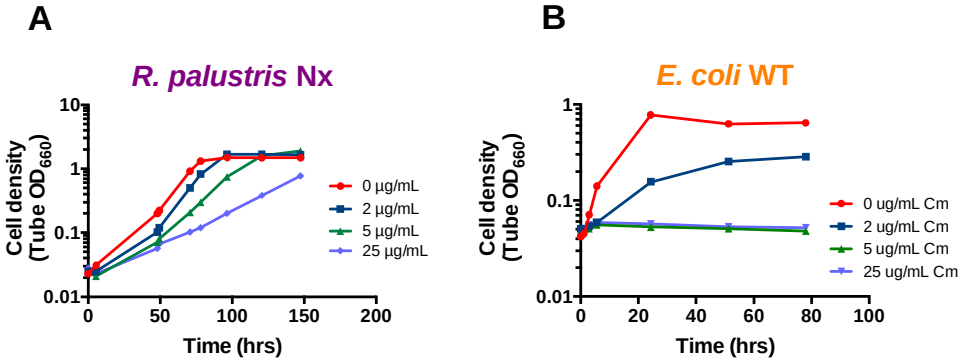

FIG S6. Determination of a chloramphenicol concentration to maintain p*amtB* in *E. coli* without harming *R. palustris*. Representative growth curves of *R. palustris* Nx (**A**) and WT *E. coli* (**B**) at different concentrations of chloramphenicol. All cultures were grown anaerobically in MDC with a 1% inoculum from stationary monocultures. *R. palustris* Nx was provided 20 mM sodium acetate as a carbon source with a 100% N_2 headspace for nitrogen. WT *E. coli* was provided 25 mM glucose, 10 mM cation solution, and 15 mM NH_4Cl.